AJDS LAZHAR Al-Azhar Journal of Dental Science Print ISSN 1110-6751 | online ISSN 2682 - 3314
Vol. 27- No. 4- 523:534- October 2024 https://ajdsm.journals.ekb.eg
Oral Biology, Medicine & Surgical Sciences Issue *(Oral Biology, Oral Pathology, Oral Periodontology, Medicine, Oral & Maxillofacial Surgery)*

WESTERN BLOT ANALYSIS OF B-LYMPHOMA MOLONEY MURINE INSERTION REGION (BMI-1) AND VASCULAR ENDOTHELIAL GROWTH FACTOR (VEGF) WHEN UTILIZING IMIQUIMOD AND/ OR BEVACIZUMAB TREATMENT ON DMBA INDUCED HAMSTER BUCCAL POUCH CARCINOMA

Amr Mahmoud Mohamed[1], Emad Soliman Mohammed El-qalshy[2], Bakheet Elkot Mostafa Elsadek [3], Mohamed Gomaa Attia Zouair[4]

ABSTRACT

Objective: Purpose of this research was to study how immunotherapy and bevacizumab affected cancer stem cell(s) (CSC(s)) in induced hamsters buccal pouch (HBP) carcinoma. **Subjects and Methods**: 50 hamsters were split into 5 groups. Animals in GI were left untreated for 19 weeks (ws), the right pouches of those belongs to (GII- GV) were painted with 7,12-dimethylbenz (a) anthracene (DMBA), 3times a week for 14 ws, then, the following was done: GII was left with no additional treatment for other 5 ws, whereas GIII was painted with imiquimod once daily for other 4 ws, Those in GIV were injected intraperitoneally (IP) with bevacizumab (10mg/kg / once daily for a week), and those in GV were painted with imiquimod similar to GIII in addition to IP injection with bevacizumab similar to GIV. Gross observations and tumor volume were recorded for each group. After slaughtering the animals, all right pouches were divided into two pieces, one of which was prepared for hematoxylin and eosin (H&E) stain. The other piece was used for western blot analysis for identification of CSCs using BMI-1stem cell marker and VEGF) antibody. **Results**: Western blot examination of BMI-1 and VEGF antibodies indicated a significantly significant (p-value < 0.001) discrepancy between GV and the subsequent; GIII and GIV. In comparison, BMI-1 showed a non-significant variation (p-value < 0.125) between GIII and GIV, but VEGF showed a very substantial difference (p-value < 0.001). **Conclusion:** Combination of imiquimod-bevacizumab has an inhibitory effect on carcinoma cell and CSCs in HBP SCC.

KEYWORDS: HBP carcinoma, imiquimod, bevacizumab, CSCs.

1. Assistant Lecturer, Oral and Dental Pathology Department, Faculty of Dental Medicine (Boys- Cairo), Al-Azhar University, Egypt.
2. Lecturer, Oral and Dental Pathology Department, Faculty of Dental Medicine (Boys- Cairo), Al-Azhar University, Egypt.
3. Assistant Professor, Department of Biochemistry and Molecular Biology, Faculty of Pharmacy, (Boys-Assiut), Al-Azhar University, Egypt.
4. Professor, Oral and Dental Pathology Department, Faculty of Dental Medicine (Boys-Cairo), Al-Azhar University, Egypt.

• ***Corresponding author*:** dramr969@gmail.com

DOI: *10.21608/ajdsm.2022.174502.1383*

INTRODUCTION

The most frequent kind of oral neoplasm is oral squamous cell carcinoma (OSCC), which accounts for more than 90% of all mouth malignancies[1]. 7,12-dimethylbenz(a)anthracene (DMBA) is a polycyclic aromatic hydrocarbon (PAH) and a powerful organ-specific procarcinogen that is often employed as a synthetic carcinogen to accelerate experimental oral carcinoma. DMBA is activated by phase I enzymes to generate diolepoxide, which oxidizes both purine bases of DNA, resulting in mutation. The DMBA-induced HBP carcinogenesis is regarded as an attractive experimental paradigm for studying natural product anticancer effects[2-5]. CSCs are a category of quiescent self renewing cell types seen in initial malignancies that have enhanced functional ability to drive tumor progression and reconstitute their heterogeneity. These cells are also linked to cancer cell development and metastasis, as well as tumor recurrence after therapy[6]. CSCs have been isolated from the majority of hematological solid tumors and malignancies, and their tumorigenesis activity has been shown in various types of cancers, including lung, brain, colon, liver, breast, pancreatic, ovarian, melanoma, prostate, and head and neck cancers, including OSCC[7].

BMI-1 is a frequent CSC marker that promotes stem cell self-renewal and has been linked to a variety of biological processes, including organ creation, embryogenesis, stem cell stability, cancer, and differentiation[8,9]. Numerous investigations have shown that BMI-1 expression is commonly increased in many kinds of human malignancies, indicating that BMI-1 may play essential roles in cancer genesis and development[10-16].

Angiogenesis is a multistep process that plays a critical role in tumor development and metastasis[17-20]. The development of potential targeted medicines has emerged from the identification of molecular pathways underpinning cancer growth, invasion, and metastatic dissemination. Anti-angiogenic therapy include the injection of VEGFR inhibitors, for example the monoclonal antibody Bevacizumab (Avastin) and other medicines, such as Cediranib and Pazopanib[21]. Bevacizumab prevents the development of new blood vessels in the tumor, eliminates present blood vessels, and reduces intertumoral pressure, allowing cytostatic medicines to penetrate deeper into the tumor. Bevacizumab has FDA approval and has been used effectively in the treatment of many forms of cancer, either alone or in combination with other chemotherapy medicines, immunology, or radiation [22-24].

Cancer immunotherapy is developing as an effective cancer treatment method that works by stimulating the immune system to achieve antitumor effects[25]. Toll-like receptors are among the pattern recognition receptors found on innate immune cells (TLRs), which are important for recognizing pathogen-associated molecular patterns and inducing an inflammatory immune response[26-28]. Imiquimod, a TLR-7 agonist, causes cytokines to be released, triggering an inflammatory skin response focused mostly towards malignant or virus-infected cells, but has little impact on healthy skin. Imiquimod 5% cream is approved by the FDA for the therapy of exterior genital warts, shallow basal cell carcinoma, and actinic keratitis, and it is being tested in a variety of additional dermato-oncological conditions[29,30], including oral dysplastic lesions or oral malignancies[31].

As a result, the primary goal of this research was to evaluate the effects of imiquimod and/or bevacizumab on DMBA-induced HBP cancer. The animals' common health exams, HBP gross inspections, histological tumor tissue alterations, and western blot analysis were used to make the determination.

SUBJECTS AND METHODS

1 Chemicals:

Sigma-Aldrich's DMBA (0.5% concentration) was dissolved in paraffin oil. Imiquimod A topical cream formulation containing 5% Imiquimod marketed by 3M pharmaceuticals as Aldara. Bevacizumab (trade name Avastin) was obtained

from Roche company dissolved in 0.9% sodium chloride (10 mg/ml)

2 Animals:

50 Syrian male hamsters weighing 80-120g were procured from Cairo University's animal home in Cairo, Egypt. A healthy hamsters had normal, effortless movement, clear eyes, bright, healthful skin, and a silky, glossy coat free of dry patches, parasites, sores, and swellings. All experiments were approved by ethical committee of Faculty of Dental Medicine, Al-Azhar University, Egypt (Ethical Code No. 148/164, 30-04-2019).

3 Experimental design:

Following one week of adaptation, the animals were divided randomly into five groups (G_s) of 10 individuals each. GII, GIII, GIV, and GV's right pouches were painted with 0.5% DMBA in liquid paraffin three times a week for fourteen weeks using a number 4 camel hair brush[32]. After that, the GII animals (positive control) were left with no additional treatment for other 5 ws (total period 19 ws), while those in GIII (imiquimod), painted with imiquimod to the injured buccal pouch once daily for other 4 ws[33], after one week (total period 19 ws), the animals of this group were euthanized. The GIV animals (bevacizumab) were injected IP by insulin syringe with VEGF inhibitor (Bevacizumab), via IP injection once daily for a week[34]. After one-week (total period 16 ws), the animals of this group were euthanized, while those in GV (imiquimod-bevacizuumab) animals received a combination of imiquimod and bevacizumab with methodologies and doses similar to those presented in the single treatments, and the animals in this group were euthanized after one week (total period 19 ws).

4 General health examinations:

The improvements in the animals' overall health were documented during the trial. When dealing with sickness or injury, hamsters displayed one or more of the following behaviors: inactivity, lack of appetite, sneezing, huddling in a corner, wheezing, and/or secretion from the nose or eyes, diarrhea, dampness around the tail, and hair loss.

2.5 Tumor volume measurement

Gross measurements were documented once the experiment was completed (exudation, mucosal thickness, tumors, and ulcers). The animals have been slaughtered, the right cheek pouch was excised, and a Vernier caliper was used to measure the diameter of each tumor. Prior to authorization, the tumor volume was computed using the formula Vmm3 = (4/3) π [(D1/2) (D2/2) (D3/2)], where D1 (height), D2 (width), and D3 (length) are the tumor's three dimensions (mm).

6 Sample collection and preparation

One piece of fresh tissue from the right cheek pouch was removed, flanked, kept in 10% neutral buffered formalin, processed, and embedded in paraffin blocks for histological analysis. The sample of fresh tissue was mechanically deteriorated, suspended, and homogenized in preparation for western blot analysis.

7 Histopathological examinations:

After being dried in an increasing ethanol series, the preserved specimens were embedded in paraffin wax to make paraffin blocks. Tissue slices were trimmed to 4m thickness, placed on glass slides, processed, and prepared for light microscopic analysis by staining with H&E.

8 Measurement of the depth of invasion (DOI):

Relying on the H&E section, DOI was calculated for all surgical specimens. DOI was calculated by measuring the distance between the basement membrane of the surface epithelium and the deepest level of the tumor nests. It is additionally separated into five mm less invasive, 6-10 mm moderately invasive, and 10 mm very invasive. According to the American Joint Committee on Cancer, Leica QWIN V3 image analysis software (Switzerland) was used to calculate DOI.

9 Western blotting assessments of BMI-1 and VEGF expression levels

The other pieces of fresh tissue specimens of HBP were collected separatly then placed in eppendorf tube and frozen with liquid nitrogen at -80°C to avoid degradation of proteins. The frozen specimens were therefore mechanically homogenized with RIPA lysis buffer (Sigma-Aldrich, Milan, Italy) comprising 1% protease inhibitor cocktail (Cell Signaling Technology, Inc., MA, USA, Cat#5871) using a Potter-Elvehjem rotor-stator homogenizer (glass/teflon homogenizer) equipped with a Teflon pestle. Homogenized tissues were frozen at -70 °C for subsequently Western blotting analysis of tissue BMI-1 and VEGF expression. The samples were then denatured in 2Laemmli buffer for 5 minutes at 95 °C before being treated with 5% 2-mercaptoethanol. SDS-PAGE electrophoresis was carried out by loading 50 g of protein per lane at 75 volts across a 10% resolving gel. This procedure was followed by 125 volts for about 2 hours, after which T-77 ECL semidry transfer equipment was used to transfer the substance to a PVDF membrane (Amersham BioSciences UK Ltd). The PVDF membrane was immunoblotted by incubating it for one hour at temperature of 4°C in TBS buffer with 0.1% Tween and 5% nonfat milk, accompanied by 24 hours of incubation at 4°C with a mouse monoclonal anti BMI-1 (Santa Cruz Biotechnology, Inc., CA, USA, Cat# sc-390443), a mouse monoclonal anti VEGF (Santa Cruz Biotechnology, Inc., CA, USA,Cat# sc-390443) and a mouse monoclonal anti VEGF (Santa Cruz Biotechnology, Inc., CA, USA, Cat# sc-53462) at a dilution of 1:1000. Following three times of washing with TBST buffer, each membrane was stored for one hour at room temperature with a dilution of 1:5000 by an alkaline phosphatase-conjugated goat anti-mouse secondary antibody (Novus Biologicals, LLC, Littleton, CO, USA, Cat# NB7536). A commercial BCIP/NBT substrate detection Kit recognized the membrane-enclosed antibody after four TBST washes (Genemed Biotechnologies, Inc., CA, USA, Cat# 10-0007) after already being washed four times in TBST. Stripping and re-blotting each membrane at 4°C with a mouse monoclonal anti-GAPDH antibody (Santa Cruz Biotechnology, Inc., CA, USA, Cat# sc-166574), equivalent protein loading for each lane was verified. The analysis was conducted three times to ensure that the findings were reproducible. The band density was quantified using ImageJ software and represented as a percentage of that of GAPDH.

10. Statistical analysis:

The outcomes were calculated and statistically examined expressed as the mean standard deviation (SD). SPSS version 17.0 for Windows was used to do a one-way analysis of variance (ANOVA). ANOVA was utilized to evaluate more than two independent groups using quantitative data and a normal distribution, followed by LSD post hoc analysis. $p > 0.05$ was deemed non-significant, $p < 0.05$ was deemed significant, and $p < 0.001$ was deemed very significant.

RESULTS

1. Gross observations:

The GI check indicated no abnormalities, hair loss, skin ulcerations, or HBP changes. All hamsters had buccal pouch lengths of around 5cm **(Fig.1A)**. GII caused significant skin ulceration, pouch depth reduction, hair loss, and overall disablement in all animals. Massive exophytic growths with apparent vasculature were seen in the pouches of the animals, which ranged in length from 1.5 to 2 cm with a distal necrotic end **(Fig.1B)**.

The overall health of GIII and GIV improved somewhat. The pouches were roughly 2.5cm long when the distal necrosis was removed. The papillomatous lesions size was reduced somewhat **(Fig.1C&D)**. GV significantly improved the animals' overall health. The length of the pouches increased to approximately 3.5cm, with no distal necrosis. In comparison to animals treated simply with imiquimod or bevacizumab, the size of exophytic aggregates was significantly reduced in these groups **(Fig.1E)**.

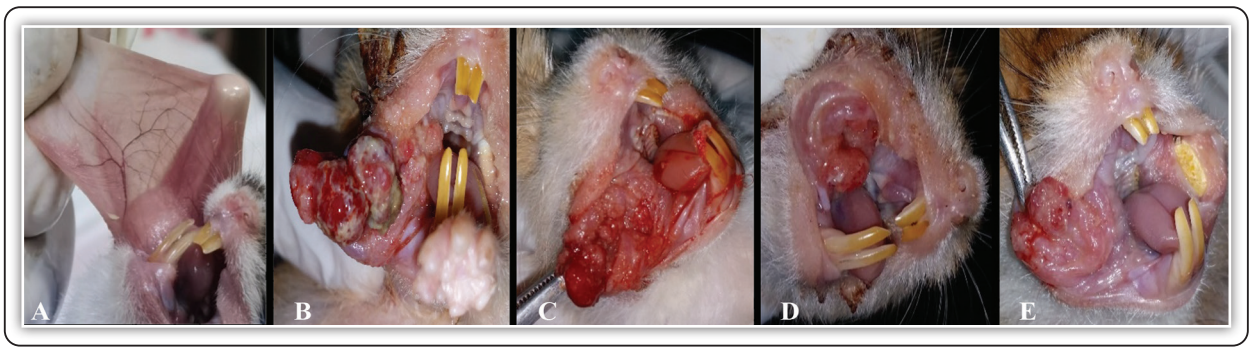

FIG (1) GI photograph of typical buccal pouch mucosa that looked pink in hue and had a smooth surface. **Fig.(1B):** Photograph of GII with multiple papillary exophytic tumor masses enclosed to bleeding areas. **Fig.(1C):** Photograph of GIII demonstrating little minor elevation with no ulceration or bleeding. **Fig.(1D):** A photograph of GIV displaying a microscopic nodule without ulceration or bleeding. **Fig.(1E):** Photograph of GV demonstrating a significant decrease in the size of tumor masses without bleeding or ulceration.

2. Histological findings:

GI examination showed typical thin layered squamous epithelium, sub-epithelial connective tissue (C.T), and muscle layer **Fig.(2A)**. GII indicated well to moderately developed SCC as vast papillomatous lesions with invasive epithelial islands into the underlying C.T. In addition, the pouch's distal end had chronic inflammatory cells and a necrotic mass. The invading epithelial cells displayed hyperchromatism, large nucleoli, an increased N/C ratio, spinous layer whirling, and nuclear and cellular pleomorphism **Fig.(2B)**. The median DOI in GII (10 hamsters) was 10.5 mm **Fig.(2C)**. In 5 hamsters, GIII and GIV showed moderate-to-severe epithelial dysplasia with top-to-bottom alterations or carcinoma in situ (CIS). The remaining 5 hamsters showed marginal invasion of well-differentiated SCC in the nodules that had not spread deeper (DOI=1.7-1.8mm). Less distal necrosis, increased inflammatory infiltration, and increased collagen fibers were seen **Fig.(2D&E)**. In seven hamsters, GV indicated moderate to severe epithelial dysplasia (epithelium had localized regions of dysplasia characterized by hyperchromatism, changed N/C ratio, nuclear & cellular pleomorphism, conspicuous nucleoli, and several group cell keratinization). In contrast, three hamsters exhibited well-differentiated SCC that has been juxtaepithelial and did not penetrate into the deeper C.T (DOI=0.8mm), there was an elevation in keratin production. The C.T revealed a significant reduction in distal necrosis, inflammation infiltration, and increased striated muscle layer thickness, and the masses of tumor were mostly displaced by fibrous connective tissue with enhanced collagen deposition **Fig.(2F)**.

3. Expressions of BMI-1 and VEGF antibodies as estimated by western blot:

A) BMI-1: When the different treatment groups (GIII, GIV, and GV) were compared, GV exhibited a very substantial difference with either GIII or GIV (p value < 0.001). In contrast, there was no statistically significant distinction between GIII and GIV (p value >0.05). When the combinations group (GV) was compared to the negative control group (GI), there was a substantial difference (p value < 0.05). The positive control group (GII) differed greatly from the treatment groups (GIII, GIV, and GV) (p value < 0.001). In contrast, no substantial difference existed between GII and GIII or GII and GIV (p value >0.05). When the control groups (GI and GII) were compared, there was a very substantial difference (p value < 0.001) **Fig. (3)**.

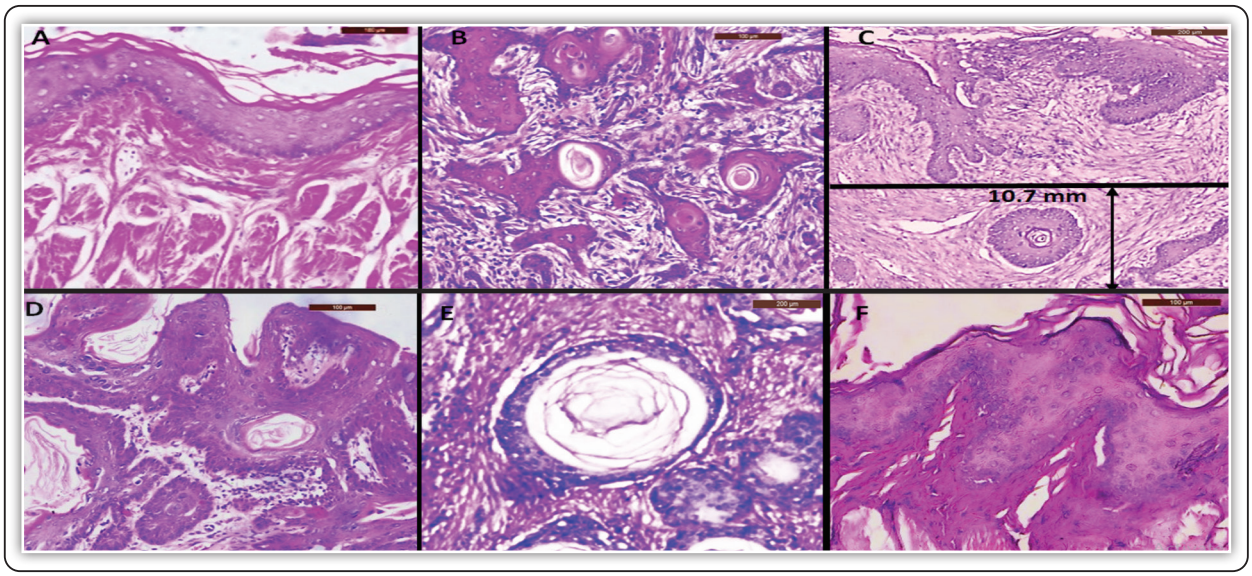

FIG. **(2A):** GI photomicrograph exhibiting 2 to 4 levels of epithelium, surface keratinized squamous cells, flattening rete ridges, C.T layer, muscle layer, and deeper layer of loose areolar connective tissue (H&E stain X400). **Fig.(2B):** Photomicrograph of GII showing highly differentiated SCC with extensive tumor island penetration into the neighboring connective tissue and subepithelial inflammatory infiltrates (H&E stain X100). **Fig.(2C):** Photomicrograph of calculating the DOI, the largest invasion was calculated by dropping a "plumb line" from the horizon to the maximum depth of the most invasive nests (H&E stain X200). **Fig.(2D):** Photomicrograph of GIII displaying SCC with well-differentiated differentiation (cursory invasion) (H&E stain X400). **Fig.(2E):** Photomicrograph of GIV showing well differentiated SCC (nests and pearls) (H&E stain X200). **Fig.(2F):** Photomicrograph of GV expressing extreme dysplasia and hyperkeratosis (H&E stain X200).

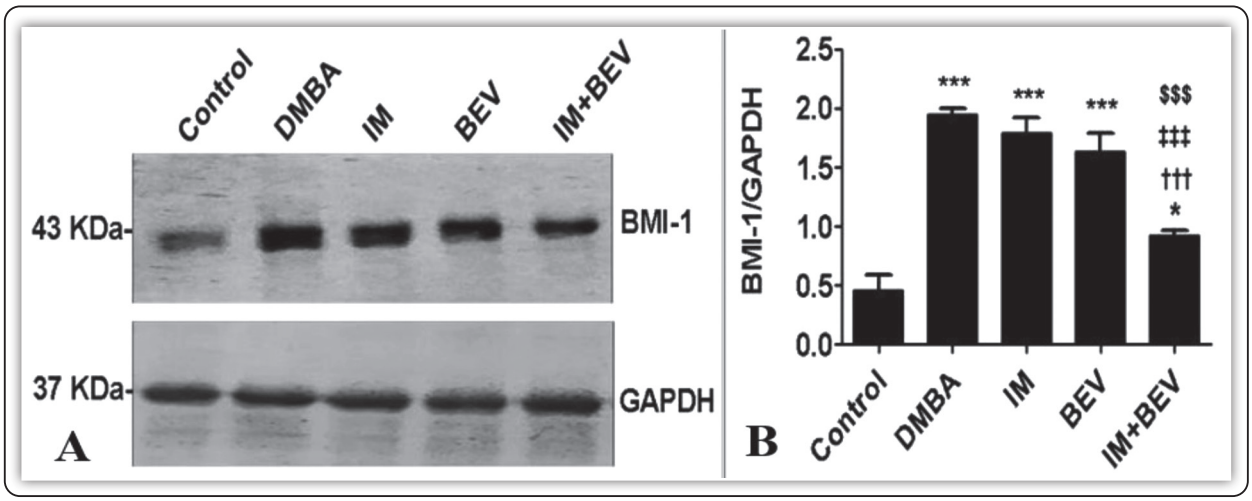

FIG. (3) Western blotting (A) and semiquantitative analysis (B) of BMI-1 protein expression in OSCC in the control and studied groups. Semiquantitative analysis was carried out by Image J® software and expressed as a percentage of GAPDH density. The data is provided as mean ±SEM (n = 6). *, †, ‡, and $ denote significant differences from control, DMBA, IM, and BEV, accordingly. *, †, ‡, and $ denote significant change at $p<0.05$; **, ††, ‡‡, and $$ denote significant difference at $p<0.01$; ***, †††, ‡‡‡, and $$$ denote massive change at $p<0.001$.

B) VEGF: Comparing the various treated groups (GIII, GIV, and GV), **GV** showed highly significant difference with either GIII or GIV (p value < 0.001). Additionally, the difference between GIII and GIV was non-significant (p value >0.05). When the combining group (GV) was compared to the negative control group (GI), there was no substantial difference (p value > 0.05). When the positive control group (GII) was compared to the different treatment groups (GIII, GIV, and GV), there was a very substantial difference (p value <0.001). In contrast, no notable change between GII and GIII or GII and GIV (p value >0.05). When the control groups (GI and GII) were compared, there was a very notable change (p value <0.001) **Fig.(4).**

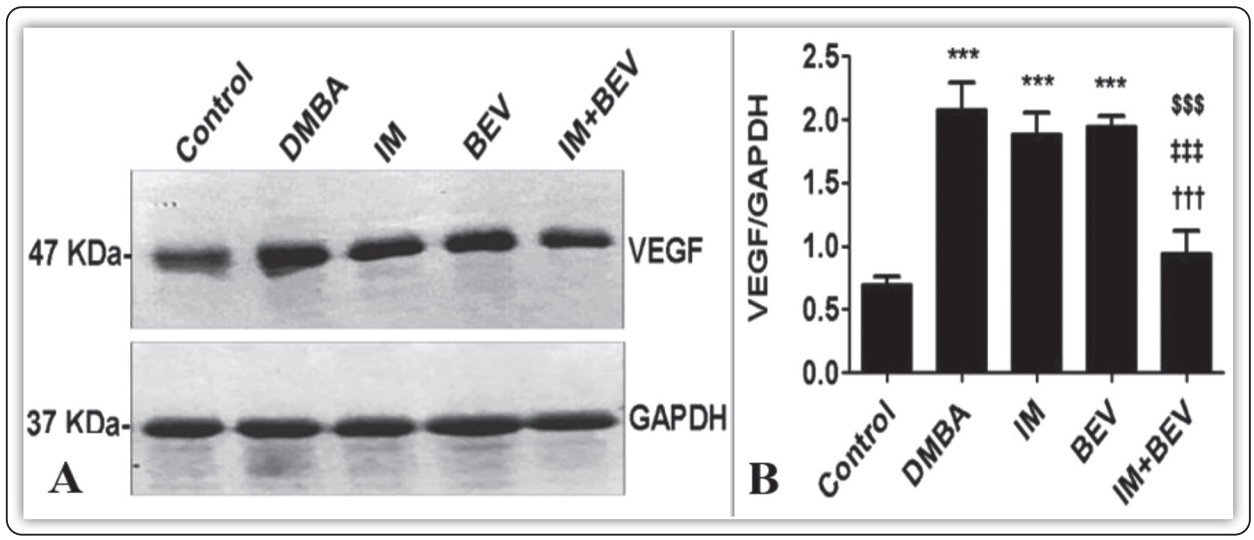

FIG. (4) Western blotting (A) and semiquantitative analysis (B) of VEGF protein expression in OSCC in the control and studied groups. Semiquantitative analysis was carried out by Image J® software and expressed as a percentage of GAPDH density. The data is provided as mean ±SEM (n = 6). *, †, ‡, and $ denote significant differences from control, DMBA, IM, and BEV, accordingly. *, †, ‡, and $ denote significant change at p<0.05; **, ††, ‡‡, and $$ denote significant difference at p<0.01; ***, †††, ‡‡‡, and $$$ denote massive change at p<0.001.

TABLE (1) Comparison between the investigated groups in terms of BMI-1 expressions

	BMI-1		P-value for post analysis using LSD test				
	Mean±SD	**Range**	**G1**	**GII**	**GIII**	**GIV**	**GV**
G I	0.48 ± 0.08	0.38 – 0.59	--	0.000	0.000	0.000	0.000
G II	1.80 ± 0.29	1.35 – 2.25	0.000	--	0.000	0.000	0.000
G III	1.70 ± 0.48	0.78 – 2.62	0.000	0.000	--	0.125	0.000
G IV	1.60 ± 0.32	1.05 – 2.15	0.000	0.000	0.125	--	0.000
G V	0.90 ± 0.14	0.65 – 1.15	0.000	0.000	0.000	0.000	--
F			**41.258**				
P-value			**<0.001 (HS)**				

TABLE (2) Comparison between the investigated groups in terms of VEGF expressions

	VEGF		P-value for post analysis using LSD test				
	Mean±SD	**Range**	**G1**	**GII**	**GIII**	**GIV**	**GV**
G I	0.70 ± 0.10	0.57 – 0.83	--	0.000	0.000	0.000	0.000
G II	2.10 ± 0.20	1.8 – 2.4	0.000	--	0.000	0.000	0.000
G III	1.70 ± 0.48	0.78 – 2.62	0.000	0.000	--	0.000	0.000
G IV	1.90 ± 0.21	1.59 – 2.21	0.000	0.000	0.000	--	0.000
G V	0.90 ± 0.14	0.65 – 1.15	0.000	0.000	0.000	0.000	--
F			**61.201**				
P-value			**<0.001 (HS)**				

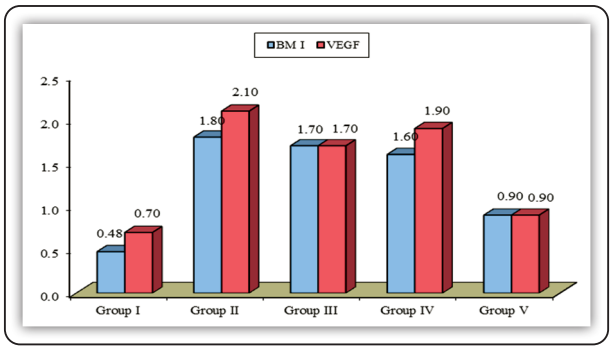

FIG (5) Comparison between the investigated groups in terms of BMI-1 and VEGF expressions.

DISCUSSION

As one of the most frequent malignancies in the globe, and despite the simple access to the oral cavity and considerable breakthroughs in therapy, the morbidity and fatality rates for people suffering from oral cancer remain quite high. The hamster cheek pouch method of oral carcinoma model is promising and significant in gaining a better knowledge of cancer biology, diagnostics, and therapy options. In the current work the results of general health observations, tumor volume, H&E stain, DOI and western blot analysis utilizing BMI-1 and VEGF antibodies showed variable insights.

In the present study, the H&E staining revealed normal histological structures This result is consistent with other investigators[3,4]. H&E stain in GII showed 50% well-differentiated and 50% moderately differentiated invasive SCC in deeper C.T. sections (DOI=10.9 mm). This is consistent with the findings of other studies[3, 5]. Balakrishnan et al (2022)[5] found that hamster cheek pouches painted with DMBA alone grew tumors at a rate of 100 percent after 14 weeks, which agrees with the current findings. This might be related to DMBA's procarcinogenic character because stage I enzymes such cytochrome P450 convert it to dihydrodiol epoxide, a carcinogen that binds to and damages DNA, leading to mutations and carcinogenesis.

In the current investigation, GIII H&E staining, which indicated that five hamsters had moderate (10%), severe (20%), or CIS (20%) epithelial dysplasia. The remaining five hamsters exhibited superficial SCC invasion (50%); however, it did not penetrate to deeper locations (DOI=1.9mm). This is consistent with previous investigations[31]. Imiquimod, when given topically, reduced tumor development. This impact was related with enhanced tumor infiltration by DC and T lymphocytes, and it was reduced by CD8+ cell depletion[28].

In the present study, almost GIV and GIII showed similar histological results. This is in line with other antiangiogenic studies [18, 23]. According to Tamura et al (2016)[35], bevacizumab caused distinctive histological alterations such as the absence of microvascular growth and a considerable decrease in microvessel density, implying normalization of the vascular structure.

In the current investigation, GV as a combination group H&E staining revealed mild (10%), moderate (30%), severe (20%), or CIS (10%) epithelial dysplasia and well-differentiated SCC (30%) that was juxta-epithelial and did not affect the deeper C.T (DOI=0.9mm) with rapid keratin production. The CT indicated increased striated muscle layer thickness and proliferating fibrous tissue with improved collagen deposition replacing tumor masses. These results indicated the advantageous impact of mixing imiquimod with bevacizumab to produce these excellent effects. Chen et al(2018)[36] shown that combining bevacizumab with immunotherapy inhibits tumor development and metastasis in human malignancies in a synergistic manner.

Western blot examination of BMI-1 in GI indicated low expression in the present research. This finding is consistent with the findings of other researchers[9, 15]. According to Park et al (2020)[15], BMI-1 is required for the self-renewal of both normal and cancer stem cells. However, the stemness genes that BMI-1 regulates are unclear.

Western blot of BMI-1 showed a significant difference between GI and GII ($p<0.001$). This supports previous studies[10, 16]. According to Paranjape et al (2014)[10], BMI-1 is required for the self-renewal of normal hematopoietic stem cells, brain stem cells, and normal mammary stem cells, and Hedgehog signaling governs self-renewal through BMI-1. However, the stemness genes that BMI-1 regulates are unclear. According to He et al (2009)[12], BMI-1 expression was linked with poor survival rate as well as lymph node metastases and clinical phase.

The link between BMI-1 overexpression and stem-like features in tumor cells might be related to the development of EMT, which increased invasion, metastasis, and poor prognosis[11]. Western blot examination of BMI-1 in the current research discovered no significant difference between GII and GIII or GII and GIV (p value >0.05). There was, however, a significantly substantial difference between GII and GV (p value < 0.001).

Furthermore, GV demonstrated a very noticeable difference with either GIII or GIV (p value < 0.001). Additionally, the difference between GIII and GIV was non-significant (p value >0.05). This finding is consistent with the findings of other researchers [24, 26]. Ren et al (2016)[26] discovered that the TLR7 agonist immunotherapy may inhibit HCC stem cell proliferation and self-renewal, an effect that might be mediated through TLR7-IKK-NFB-IL6 signaling. Bevacizumab, a VEGF tyrosine kinase inhibitor, has been shown to extend life time in glioblastoma by targeting the perivascular niche[24].

Western blot examination of VEGF in the present research revealed a considerable difference between GI and GII (p value < 0.001). This supports previous studies[19, 20]. VEGF clearly has a function in embryonic angiogenesis as well as physiological angiogenesis activities, such as corpus luteum formation and wound healing. VEGF is expressed in the embryo as well as numerous adult human and mouse organs, including the adrenal gland, kidney, lung, and heart. Lin et al (2019)[20] discovered a considerable rise in VEGF expression during shift between normal and OSCC tissues, which correlates with increased differentiation degree.

Western blot analysis of VEGF revealed no significant changes between GII and GIII or GIV ($p > 0.05$). However, GII and GV differed substantially ($p < 0.001$). GV also differed significantly from GIII or GIV ($p < 0.001$). Moreover, GIII-GIV difference was non-significant (p value >0.05). This finding is consistent with the findings of other researchers [27,30]. Hashemi et al (2018)[30] discovered that tumor cells

express several powerful angiogenic molecules, including VEGF, angiogenin, fibroblast growth factor, and IL-8, which stimulate angiogenesis, which is essential for tumor development and invasiveness. Tumor cell eradication may thereby lower the number of tumor-derived substances, particularly proangiogenic factors, directly.

Damiano et al (2007)[27] found that the combination of TLR agonist and bevacizumab reduces hVEGF levels but just not mVEGF levels. Their findings imply that the murine-dependent immune-mediated actions of TLR agonists improve bevacizumab activity on tumor cells. They found that TLR agonists reduce endothelial cell proliferation, adherence, and migration, as well as VEGF-stimulated capillary tube and networks development.

In the present study, there was a statistically significant positive (direct) correlation either between BMI-1 and VEGF (p value>0.001) or between tumor volume and both of BMI-1 & VEGF expressions respectivly (p value>0.001). This indicates that a rise in one variable causes an increase in the other, and vice versa.

These findings show that BMI-1 plays a role in cancer invasiveness via modulating the expression of PTEN and vascular endothelial growth factors[37]. BMI-1 knockdown lowered the expression and activity of MMP-2, MMP-9, and VEGF, according to Li et al (2013)[13]. These findings imply that knocking down BMI-1 limits HCC cell invasion by suppressing MMP-2, MMP-9, and VEGF. Meng et al (2012)[14] found that knocking down BMI-1 reduces lung cancer cell migration and metastasis by reducing VEGF production through the PTEN/PI3K/Akt signaling pathway.

CONCLUSION

This research discovered that CSCs may promote tumor development by immunoediting CSCs to allow them to live in immunocompetent hosts or by creating circumstances that promote neoplastic growth inside the tumor microenvironment. Our results demonstrated that combination of imiquimod-bevacizumab has an inhibitory effect on tumor progression in OSCC, which was found to be more efficient than either agent alone. Regarding efficacy, a (10 mg/ml) of bevacizumab once daily for a week combined with 5% imiquimod once daily for 4 weeks afford a prominent respons rate, which was evident in terms of gross observation, tumor volume, histopathological examination, DOI and western blot analysis utilizing BMI-1 and VEGF antibodies. As a consequence, future immunotherapeutic targeting of CSCs may improve efficacy and durability. Accordingly, Further studies to be carried out on the same model, with increase concentration or dose of the used drugs and/or change the way of administration.

REFERENCES

1. Jiang X, Wu J, Wang J, Huang R. Tobacco and oral squamous cell carcinoma: A review of carcinogenic pathways. Tob Induc Dis. 2019;17:29.
2. Babukumar S, Vinothkumar V, Velu P, Ramachandhiran D. Hesperetin on cell surface glycoconjugates abnormalities and immunohistochemical staining with cytokeratin in 7, 12 dimethylbenz (a) anthracene induced Hamster Buccal pouch carcinogenesis. Indian J Clin Biochem. 2018;33(4):438-44.
3. Shamia A, Abd-Alhafez A, Al-qalshy E, Zouair M. Therapeutic efficacy of time-dependent cetuximab on experimentally induced hamster buccal pouch carcinoma. Int J Health Sci. 2022;6(S5):3431-3456.
4. Ezzat S, AbuElkhair M, Mourad M, Helal M, Grawish M. Effects of aqueous cinnamon extract on chemically-induced carcinoma of hamster cheek pouch mucosa. Biochem Biophys Rep. 2017; 12: 72–78.
5. Balakrishnan V, Ganapathy S, Veerasamy V, Duraisamy R, Sathiavakoo V, Krishnamoorthy V, et al. Anticancer and antioxidant profiling effects of Nerolidol against DMBA induced oral experimental carcinogenesis. J Biochem Mol Toxicol. 2022;36(6):e23029.
6. Yang L, Shi P, Zhao G, Xu J, Peng W, Zhang J, et al. Targeting cancer stem cell pathways for cancer therapy. Signal Transduct Target Ther. 2020;5(1):1-35.

7. Najafi M, Farhood B, Mortezaee K. Cancer stem cells (CSCs) in cancer progression and therapy. J Cell Physiol. 2019;234(6):8381-95.
8. Curtarelli R, Gonçalves J, Dos-Santos L, Savi M, Nör J, Mezzomo L, et al. Expression of cancer stem cell biomarkers in human head and neck carcinomas: a systematic review. Stem cell reviews and reports 2018;14(6):769-84.
9. Wang J, Xing Y, Wang Y, He Y, Wang L, Peng S, et al. A novel BMI-1 inhibitor QW24 for the treatment of stem-like colorectal cancer. J Exp Clin Cancer Res. 2019;38(1):1-4.
10. Paranjape A, Balaji S, Mandal T, Krushik E, Nagaraj P, Mukherjee G,et al. Bmi1 regulates self-renewal and epithelial to mesenchymal transition in breast cancer cells through Nanog. BMC cancer 2014;14(1):1-4.
11. Chou C, Yang N, Liu T, Tai S, Hsu D, Chen Y, et al. Chromosome Instability Modulated by BMI1–AURKA Signaling Drives Progression in Head and Neck CancerBM11-AURKA Axis in Cancer Progression. Cancer Res. 2013;73(2):953-66.
12. He X, Cao X, Ji L, Zhu B, Lv J, Wang D, et al Association between Bmi1 and clinicopathological status of esophageal squamous cell carcinoma.World J Gastroenterol. 2009;15(19):2389.
13. Li X, Yang Z, Song W, Zhou L, Li Q, Tao K,et al. Overexpression of Bmi-1 contributes to the invasion and metastasis of hepatocellular carcinoma by increasing the expression of matrix metalloproteinase (MMP)-2, MMP-9 and vascular endothelial growth factor via the PTEN/PI3K/Akt pathway. Int J Oncol. 2013;43(3):793-802.
14. Meng X, Wang Y, Zheng X, Liu C, Su B, Nie H, et al. shRNA-mediated knockdown of Bmi-1 inhibit lung adenocarcinoma cell migration and metastasis. Lung Cancer 2012;77(1):24-30.
15. Park K, Ok C, Jang H, Bae M, Bae S. Resveratrol inhibits cell growth via targeting the Bmi-1 pathway in YD-10B human oral squamous cell carcinoma cells. Int J Oral Biol. 2020;45(3):115-25.
16. Xu Z, Zhou Z, Zhang J, Xuan F, Fan M, Zhou D, et al. Targeting BMI-1-mediated epithelial-mesenchymal transition to inhibit colorectal cancer liver metastasis. Acta Pharm Sin B. 2021;11(5):1274-85.
17. Aspriţoiu V, Stoica I, Bleotu C, Diaconu C. Epigenetic Regulation of Angiogenesis in Development and Tumors Progression: Potential Implications for Cancer Treatment. Front Cell Dev Biol. 2021:2462.
18. Juanes C, Souza S, Braga V, Barreto F, Aguiar G, Pimentel K, et al. Red propolis and L-lysine on angiogenesis and tumor growth in a new model of hamster cheek pouch inoculated with Walker 256 tumor cells. Einstein (São Paulo) 2019;17.
19. Araki-Maeda H, Kawabe M, Omori Y, Yamanegi K, Yoshida K, Yoshikawa K, et al. Establishment of an oral squamous cell carcinoma cell line expressing vascular endothelial growth factor a and its two receptors. J Dent Sci. 2022 ;17(4):1471-9.
20. Lin Y, Huang S, Wu J, Chu T, Huang S, Lee C, et al. Novel HDGF/HIF-1α/VEGF axis in oral cancer impacts disease prognosis. BMC cancer 2019;19(1):1-2.
21. Kong D, Kim M, Jang J, Na H, Lee S. A review of anti-angiogenic targets for monoclonal antibody cancer therapy. Int J Mol Sci. 2017 Aug 17;18(8):1786.
22. Xu R, Muro K, Morita S, Iwasa S, Han S, Wang W, et al. Modified XELIRI (capecitabine plus irinotecan) versus FOLFIRI (leucovorin, fluorouracil, and irinotecan), both either with or without bevacizumab, as second-line therapy for metastatic colorectal cancer (AXEPT): a multicentre, open-label, randomised, non-inferiority, phase 3 trial. Lancet Oncol. 2018;19(5):660-71.
23. Itashiki Y, Harada K, Takenawa T, Ferdous T, Ueyama Y, Mishima K. Antitumor effects of bevacizumab in combination with fluoropyrimidine drugs on human oral squamous cell carcinoma. Oncol Lett. 2021;22(4):730.
24. Zhang J, Xue W, Xu K, Yi L, Guo Y, Xie T, et al. Dual inhibition of PFKFB3 and VEGF normalizes tumor vasculature, reduces lactate production, and improves chemotherapy in glioblastoma: insights from protein expression profiling and MRI. Theranostics 2020;10(16): 7245-59.
25. Yu Y, Cui J. Present and future of cancer immunotherapy: A tumor microenvironmental perspective. Oncol Lett. 2018;16(4):4105-13.
26. Ren X, Wang F, Ji B, Gao C. TLR7 agonist induced repression of hepatocellular carcinoma via the TLR7-IKK-NF-ϰB-IL6 signaling pathway. Oncol Lett. 2016;11(5):2965-70.
27. Damiano V, Caputo R, Garofalo S, Bianco R, Rosa R, Merola G, et al. TLR9 agonist acts by different mechanisms synergizing with bevacizumab in sensitive and cetuximab-resistant colon cancer xenografts. Proc Natl Acad Sci U S A. 2007;104(30):12468-73..
28. Mäkinen L, Atula T, Häyry V, Jouhi L, Datta N, Lehtonen S, et al. Predictive role of Toll-like receptors 2, 4, and 9 in oral tongue squamous cell carcinoma. Oral Oncol. 2015;51(1):96-102.

29. Ren S, Wang Q, Zhang Y, Song Y, Dong X, Zhang W, et al. Imiquimod enhances the potency of an exogenous BM-DC based vaccine against mouse melanoma. Int Immunopharmacol. 2018;64:69-77.
30. Hashemi A, Hashemi H, Kahnamouii S, Hashemi T, Agajani H, Frozannia K, et al. Activation Toll-Like Receptor7 (TLR7) Responsiveness Associated with Mitogen-Activated Protein Kinase (MAPK) Activation in HIOEC Cell Line of Oral Squamous Cell Carcinoma. J Dent (Shiraz) 2018;19(3):217.
31. Camargo L, Remiro P, Rezende G, Santos S, Franz-Montan M, Moraes Â. Development of bioadhesive polysaccharide-based films for topical release of the immunomodulatory agent imiquimod on oral mucosa lesions. Eur Polym J. 2021;151:110422.
32. Vinoth A, Kowsalya R. Chemopreventive potential of vanillic acid against 7, 12-dimethylbenz (a) anthracene-induced hamster buccal pouch carcinogenesis. J Cancer Res Ther. 2018;14(6):1285-90.
33. Ruiz-Villaverde R, Sanchez-Cano D, Burkhardt-Perez P. Superficial basal cell carcinoma treated with imiquimod 5% topical cream for a 4-week period: a case series. J Eur Acad Dermatol Venereol. 2009;23(7):828-31.
34. Yasuda S, Sho M, Yamato I, Yoshiji H, Wakatsuki K, Nishiwada S, et al. Simultaneous blockade of programmed death 1 and vascular endothelial growth factor receptor 2 (VEGFR2) induces synergistic anti-tumour effect in vivo. Clin Exp Immunol. 2013;172(3):500-6.
35. Tamura R, Tanaka T, Miyake K, Tabei Y, Ohara K, Sampetrean O, et al. Histopathological investigation of glioblastomas resected under bevacizumab treatment. J Oncot. 2016;7(32):5423-35.
36. Chen D, Hurwitz H. Combinations of bevacizumab with cancer immunotherapy. Cancer J. 2018;24(4):193-204.
37. Vlachostergios P, Papandreou C. The Bmi-1/NF-κB/VEGF story: another hint for proteasome involvement in glioma angiogenesis?. J Cell Commun Signal. 2013;7(4):235-37.